

1 **Surface temperature effects of recent reductions in shipping**  
2 **SO<sub>2</sub> emissions are within internal variability**

Deleted: Weak surface

Deleted: , with quantification confounded by

3 Duncan Watson-Parris<sup>1</sup>, Laura J. Wilcox<sup>2</sup>, Camilla W. Stjern<sup>3</sup>, Robert J. Allen<sup>4</sup>, Geeta Persad<sup>5</sup>,  
4 Massimo A. Bollasina<sup>6</sup>, Annica M. L. Ekman<sup>7</sup>, Carley E. Iles<sup>3</sup>, Manoj Joshi<sup>8</sup>, Marianne T.  
5 Lund<sup>3</sup>, Daniel McCoy<sup>9</sup>, and Daniel M. Westervelt<sup>10</sup>, Andrew Williams<sup>11</sup>, Bjørn H. Samset<sup>3</sup>

6 <sup>1</sup>Scripps Institution of Oceanography and Halıcıoğlu Data Science Institute, UC San Diego

7 <sup>2</sup>National Centre for Atmospheric Science, Department of Meteorology, University of Reading

8 <sup>3</sup>CICERO Center for International Climate Research, Oslo

9 <sup>4</sup>Department of Earth and Planetary Sciences, University of California, Riverside

10 <sup>5</sup>Jackson School of Geosciences, University of Texas at Austin

11 <sup>6</sup>School of GeoSciences, University of Edinburgh, UK

12 <sup>7</sup>Department of Meteorology and Bolin Centre for Climate Research, Stockholm University

13 <sup>8</sup>Climatic Research Unit, School of Environmental Sciences, University of East Anglia, UK

14 <sup>9</sup>University of Wyoming

15 <sup>10</sup>Lamont-Doherty Earth Observatory, Columbia University

16 <sup>11</sup>Princeton University

17 *Correspondence to:* Duncan Watson-Parris (dwatsonparris@ucsd.edu)

18 **Abstract.**

19 In 2020 the International Maritime Organization (IMO) implemented strict new regulations on the emissions of  
20 sulphate aerosol from the world's shipping fleet. This can be expected to lead to a reduction in aerosol-driven  
21 cooling, unmasking a portion of greenhouse gas warming. The magnitude of the effect is uncertain, however, due  
22 to the large remaining uncertainties in the climate response to aerosols. Here, we investigate this question using  
23 an 18-member ensemble of fully coupled climate simulations evenly sampling key modes of climate variability  
24 with the NCAR CESM2 model. We show that while there is a clear physical response of the climate system to the  
25 IMO regulations, including a surface temperature increase, we do not find global mean temperature influence that  
26 is significantly different from zero. The 20-year average global mean warming for 2020-2040 is +0.03 °C, with a

29 5-95% confidence range of [-0.09, 0.19], reflecting the weakness of the perturbation relative to internal variability.  
30 We do, however, find a robust, non-zero regional temperature response in part of the North Atlantic. We also find  
31 that the maximum annual-mean ensemble-mean warming occurs around a decade after the perturbation in 2029,  
32 which means that the IMO regulations have likely had very limited influence on observed global warming to date.  
33 We further discuss our results in light of other, recent publications that have reached different conclusions. Overall,  
34 while the IMO regulations may contribute up to 0.16 °C [-0.17, 0.52] to the global mean surface temperature in  
35 individual years during this decade, consistent with some early studies, such a response is unlikely to have been  
36 discernible above internal variability by the end of 2023 and is in fact consistent with zero throughout the 2020-  
37 2040 period.

## 38 **Introduction**

39 Anthropogenic aerosols play a complex and dual role in Earth's climate system. On the one hand, they contribute  
40 to atmospheric pollution, adversely affecting air quality and public health. On the other hand, they mostly exert a  
41 net cooling effect on the climate by increasing the albedo, or reflectivity, of the atmosphere, thereby reducing the  
42 amount of solar radiation that reaches the Earth's surface (Bellouin et al., 2020). Sulphate aerosols, for instance,  
43 scatter sunlight, directly and enhance cloud brightness by increasing the number of water droplets in clouds, further  
44 reflecting sunlight away from the Earth (e.g. Albrecht, 1989; Twomey, 1974). Anthropogenic aerosol emissions  
45 thereby currently induce a global average cooling which (partially) offsets greenhouse gas driven warming by  
46 around 0.5 [0.22 to 0.96] °C compared to pre-industrial times (Forster et al., 2021). The magnitude of aerosol  
47 cooling is a key uncertainty in climate science and hinders our ability to accurately predict the magnitude and  
48 timing of future warming (Watson-Parris & Smith, 2022).

Deleted: at

50 Environmental and health concerns associated with anthropogenic aerosols have led to international efforts to  
51 reduce their emission, with potentially significant consequences for the climate (Wall et al., 2022). In January  
52 2020, the International Maritime Organization (IMO) took a significant step in this direction by implementing  
53 stringent regulations to curb sulphur dioxide (SO<sub>2</sub>; a precursor for sulphate aerosol) emissions from the global  
54 shipping fleet (IMO 2019), which at the time contributed around 14% of all anthropogenic sources of these  
55 pollutants (Christensen et al., 2022). Given the substantial share of global trade transported by sea, and the  
56 corresponding volume of emissions from shipping, the impact of these regulations on the global climate system  
57 was anticipated to be notable, and to provide a useful experiment to quantify broader aerosol impacts (Christensen  
58 et al., 2022). Similar regulatory efforts in other sectors, and national efforts in major industrial nations such as  
59 China (Li et al., 2017; Samset et al., 2019; van der A et al., 2017), also aim to improve air quality by reducing  
60 emissions of SO<sub>2</sub> and other aerosol precursors or species, thereby posing a challenge to climate scientists: to  
61 quantify and predict how these reductions will influence Earth's energy balance and the ongoing rate and pattern  
62 of warming.

63 While focussed studies have found evidence of the effect of the change in shipping emissions on cloud brightness  
64 (Diamond, 2023; Watson-Parris et al., 2022), it is challenging to discern any signal in large-scale cloud properties  
65 because the observed covariability does not always flow causally from the observed microphysical properties  
66 (Glassmeier et al., 2021; Stevens & Feingold, 2009). The instantaneous radiative forcing due to aerosol-cloud  
67 interactions from the 2020 change in shipping emissions is estimated to be 0.5 W m<sup>-2</sup> in the annual mean within  
68 shipping corridors (Diamond, 2023). Best estimates of the global mean effective radiative forcing (ERF) resulting  
69 from an 80% drop in shipping emissions range from 0.035 to 0.15 W m<sup>-2</sup> across multiple models and methodologies  
70 (Gettelman et al. 2024; Skeie et al., 2024; Yoshioka et al., 2024). Yuan et al. (2024) report a forcing of 0.2 W m<sup>-2</sup>  
71 averaged over the global ocean only, which is consistent with these global estimates.

72

73 A possible discernible climate influence of the IMO regulations became a topic for discussion in 2023, when  
74 observed global mean surface temperatures (GMST) set a record. The 2023 GMST anomaly exceeded predictions  
75 based on long-term climate change trends and internal variability, including the El Niño-Southern Oscillation  
76 (ENSO), by more than 0.2°C, causing speculation that the reduction in SO<sub>2</sub> emissions from shipping could be one  
77 of the driving factors (Schmidt, 2024). Based on the estimates of ERF given above, however, calculations with  
78 simple energy balance models (EBMs) suggest that the warming associated with shipping changes since 2020 is  
79 unlikely to exceed 0.05 °C by 2023, with a long-term response of 0.07°C (Gettelman et al., 2024). A weakness of  
80 the EBMs in this case, however, is that they generally assume a spatially homogeneous forcing and thus cannot  
81 account for the spatial heterogeneity in ocean feedbacks or climate responses to aerosol forcing, which is known  
82 to be substantial (Persad & Caldeira, 2018; Shindell & Faluvegi, 2009; Westervelt et al., 2020).

83

84 To provide a quantitative estimate of the magnitude and pattern of the climate response to the IMO shipping  
85 regulations, and the role it may have played in recent record surface temperatures, it is therefore crucial to also  
86 have estimates using fully coupled Earth System Models (ESMs), that take into account a broad range of aerosol-  
87 climate interactions and their spatial heterogeneity, as well as internal variability and its potential feedback on  
88 transient climate forcing. The latter means that it is necessary to use an ensemble of model simulations that is  
89 sufficiently large to discern a statistically significant temperature response to a weak perturbation. Even with  
90 ESMs, structural uncertainty and ensemble size create disagreement, as evidenced by recent studies of surface  
91 warming estimates due to shipping emission reductions. For instance, Yoshioka et al. (2024) found a global mean  
92 temperature increase of 0.04°C, averaged over 2020 to 2049, in response to a 0.13 W m<sup>-2</sup> ERF in HadGEM3-

Deleted: 07K

Deleted: ).

Deleted: 04K,

96 GC3.1, while Quaglia & Visoni (2024) found a global temperature increase of 0.2 °C by 2030 in response to an  
97 approximately 0.2 W m<sup>-2</sup> radiative perturbation in CESM2 (for a 90% reduction in shipping emissions).

Deleted: ERF

98  
99 Here, we present estimates of the transient surface temperature implications of the recent IMO regulations, using  
100 a large (18 member) ensemble of fully coupled transient simulations with the Community Earth System Model  
101 version 2 (CESM2). We show the ensemble mean response over time and discuss the implications of the sample  
102 size for the ability to quantify any forced warming. Also, as it is conceivable that the current specific phases of  
103 ENSO and Atlantic Multi-decadal Oscillation (AMO) could be particularly (in)sensitive to radiative perturbations  
104 in the shipping corridors (e.g. Wang et al., 2022), we have designed the ensemble to sample different modes of  
105 climate variability. Finally, as there have already been a range of studies quantifying the temperature response to  
106 the IMO regulations leading to differing, if not opposite, conclusions, we provide a broader discussion on the  
107 challenges and limitations of disentangling the effect of shipping emissions using currently available climate  
108 modelling methodologies.

## 109 **Methods**

110 CESM2 (Danabasoglu et al., 2020) consists of the Community Atmosphere Model version 6 (CAM6; Bogenschutz  
111 et al., 2018), the Parallel Ocean Program version 2 (POP2; Danabasoglu et al., 2012), the Community Land Model  
112 version 5 (CLM5; Lawrence et al., 2019), and the Community Ice Code version 5 (CICE; Hunke et al., 2015).  
113 Aerosols in CAM6 are represented by the four-mode version of the Modal Aerosol Module (MAM4; Liu et al.,  
114 2016). We note that 2.5% of SO<sub>2</sub> emissions from the international shipping sector are emitted as sulphate aerosol  
115 at the surface level and into the accumulation mode (Emmons et al., 2020). The cloud microphysics scheme is

117 version 2 of the Morrison-Gottelman scheme (Gottelman & Morrison, 2015). Simulations are performed at  
118 approximately 1° horizontal resolution.

119

120 Our baseline experiments come from archived simulations performed as part of the CESM2 Large Ensemble  
121 (CESM2-LE) Project (Rodgers et al., 2021). From 2015 onwards, CESM2-LE uses aerosol/precursor gas  
122 emissions (including SO<sub>2</sub>/SO<sub>4</sub> from international shipping), land use changes, and greenhouse gas concentrations  
123 from the Shared Socioeconomic Pathway 3-7.0 (SSP3-7.0; O'Neill et al., 2016). Our perturbation experiments are  
124 initialised from the CESM2-LE baseline experiments beginning in 2015 and integrated through 2040. The  
125 perturbation simulations are identical to the baseline simulations, except for a uniform 80% reduction in SO<sub>2</sub>/SO<sub>4</sub>  
126 emissions from international shipping starting in 2020 (consistent with the IMO regulations) and extending through  
127 2040. Thus, taking a difference (perturbation minus baseline) isolates the effects of the decrease in SO<sub>2</sub> emissions  
128 from international shipping.

129

130 CESM2 has a relatively strong anthropogenic aerosol forcing when quantified in isolation, and a high climate  
131 sensitivity compared to other ESMs (see Figure 1; Schlund et al., 2020; Zelinka et al., 2023). Its oceanic response  
132 has also been shown to be particularly sensitive to aerosol emissions (Fasullo et al., 2023; Hassan et al., 2021).  
133 For this particular perturbation however, CESM2 shows a similar radiative forcing to other ESMs (Skeie et al.,  
134 2024). Our model setup is the same as the one used for CESM2 in Gottelman et al. 2024 who report an ERF of  
135 0.11 Wm<sup>-2</sup> for a 100±25% reduction in shipping SO<sub>2</sub> emissions. This places CESM2 near the mean of the ERF  
136 estimates recently provided (Skeie et al., 2024; Gottelman et al. 2024).

137

138 To help understand the possible importance of the imposed shipping emissions perturbation relative to internal  
139 climate variability, we perform 18 ensemble simulations. These ensemble members all use CESM2-LE  
140 realisations that feature 11-year running mean smoothed CMIP6 biomass burning emissions, including members  
141 1011-001, 1031-002, 1051-003, 1091-005, 1111-006, 1131-007, 1151-008, 1171-009, 1191-010, 1231-011, 1231-  
142 012, 1231-016, 1231-018, 1251-012, 1281-017, 1281-020, 1301-015, 1301-017. All comparisons and differences  
143 are calculated with respect to the 18 corresponding unperturbed ensemble members. Recent satellite data  
144 introduces more interannual variability into the biomass burning dataset than data sources used before 1997 and  
145 after 2014, so smoothing reduces the variability in biomass burning fluxes over 1990–2020 (Fasullo et al., 2022).  
146 Furthermore, to help understand the possible importance of dominant modes of climate variability (e.g., ENSO  
147 and AMV) to the climate impacts associated with the shipping perturbation, 8 of the above ensemble members  
148 feature ENSO neutral conditions, 5 feature ENSO positive conditions and 5 feature ENSO negative conditions.  
149 The AMV index is also evenly sampled in the ensemble, for each ENSO state, and spans -0.15 to 0.15.

150

151 The simulated responses are compared to observed SST changes, diagnosed from the HadCRUT v5.0.2 analysis  
152 (Morice et al., 2021). We fit a locally weighted regression (LOESS) model over time to each 5x5 degree grid-cell  
153 to model the long-term SST trends (2020-2040), and then subtract this to discern the anomaly in 2023.

154

155 In the following, unless otherwise specified, estimates for surface temperature change are for the period 2020-  
156 2040. All significance tests are performed using a two-sided Student's t-test for the null hypothesis that two  
157 independent samples (drawn from two distributions with equal variance) have identical average (expected) values.

Deleted: .

159 **Results**

160 Figure 2a shows the relative change in near-surface SO<sub>2</sub> concentration in the reduction scenario compared to  
161 baseline and demonstrates that the majority of the changes in near-surface SO<sub>2</sub> occur over the Northern Hemisphere  
162 oceans and in particular over the North Atlantic and North-East Pacific – clearly aligned with the main international  
163 shipping routes. Figure 2b shows the change in near-surface SO<sub>2</sub> concentrations over the simulation period both  
164 globally and over the North Atlantic. The gradual reduction in the change over the period is due to the underlying  
165 shipping emission reductions in the baseline SSP3-7.0 scenario.

166

167 Despite these wide-spread and regionally significant changes in SO<sub>2</sub> concentrations (and corresponding SO<sub>4</sub>

168 concentrations, not shown), the temperature response in these simulations is negligible. Based on our sample of

169 18 simulations, we calculate a global, 20-year mean surface temperature change from the IMO regulations of +0.03

170 °C, with a 5-95% confidence range of [-0.09, 0.19]. Figure 3a shows the temperature change with respect to the

171 baseline simulations as a global mean and over the North Atlantic, neither of which show significant spatial-mean

172 warming over the 20-year study period. In fact, over the first five years there is no statistically robust change in

173 temperature found anywhere on the globe (see Fig 3b), demonstrating the low strength of the perturbation with

174 respect to the model's simulated internal variability of the Earth system. Averaging over 20 years, a robust

175 localized signal starts to appear during 2020-2040 in a small region of the North Atlantic (see Fig 3c) where there

176 is a statistically significant local warming of around 0.2°C. Figure 3d shows that the anomalous warming observed

177 in the region in 2023 (see Methods) does broadly correspond with the pattern of simulated warming in response to

178 the IMO regulations, but only as discerned after 20 years, visualised in Fig. 3e (which is a close-up of 3c).

179

Deleted: ),

Deleted: °C,



182 Despite some degree of similarity between the recent observed anomalous warming and the simulated temperatures  
183 shown in Fig 3e, the timescales do not match. The observed anomalies occurred three years after the emissions  
184 changes, while the average model response over the first five years (2020-2025) shows no significant warming in  
185 the region (Fig. 3b). As noted above, it is possible that the particular phase of ENSO or AMO could have made  
186 the North Atlantic particularly susceptible to such a perturbation in this short period of time in observations, but  
187 by sub-sampling our ensemble based on these characteristic modes we still find no evidence that the shipping  
188 emissions changes could have contributed significantly to the observed global temperature changes (see Fig. 4).

Deleted: ).

189  
190 As mentioned above, detecting the climate impacts of a relatively small externally forced perturbation, such as the  
191 estimated global top-of-atmosphere radiative forcing associated with the IMO shipping regulations (e.g., +0.12 +/-  
192 0.03 Wm<sup>-2</sup>; Gettelman et al. 2024), is complicated by the influence of internal climate variability (Deser et al.,  
193 2012, 2020). Figure 5 shows the actual evolution of our 18 ensemble members, with and without the IMO  
194 regulations, compared to the HadCRUT5 global surface temperature anomaly data series. The observed evolution  
195 is clearly within the range sampled by CESM2, in both emission scenarios. This difficulty is compounded over  
196 smaller (e.g., regional) spatial scales and shorter (e.g., decadal) time scales. The ability to robustly separate and  
197 quantify a forced signal in the climate system is the goal and motivation of “large-ensembles” (e.g. Kay et al.,  
198 2015; Kirchmeier-Young et al., 2017; Maher et al., 2019; Rodgers et al., 2021; Simpson et al., 2023), whereby  
199 dozens or more independent climate model ensemble members are generated using identical external forcing but  
200 different initial climate states. Since ensemble members will in general feature different timing of internal climate  
201 variability—which essentially represents noise (i.e., the component of the signal that is not externally forced)—  
202 averaging over a larger number of ensemble members reduces such noise, allowing for a more robust quantification  
203 of the externally forced signal.

205

206 Figure 6 shows the important influence of internal climate variability to the global mean temperature response ( $\Delta T$ )  
207 in our CESM2 shipping perturbation experiments, as well as the importance of having a sufficient ensemble size  
208 to robustly detect a forced response. Fig. 6a shows the impact of randomly selecting  $N$  of our 18 ensemble  
209 members with replacement (i.e. a bootstrapping analysis). For each combination we calculate the corresponding  
210 ensemble global mean temperature response. The figure shows the results from 1000 samples. For small  $N$ , the  
211 spread in the ensemble mean  $\Delta T$  is quite large (approximately  $-0.09$  to  $0.125$  °C for  $N = 5$ ). For  $N = 10$ , the spread  
212 is reduced, but it still exceeds  $\pm 0.05$  °C. As  $N$  continues to increase, however, the spread converges to our 18-  
213 ensemble member  $\Delta T$ .

214

215 To further illustrate the importance of ensemble size when dealing with perturbations that have weak responses  
216 relative to internal variability, Figure 6b-d show example combinations of 10 unique ensemble members (as used  
217 e.g. by Quaglia & Visioni, 2024). Statistical testing and hatching is done as for our Figure 3 (see Methods). Fig.  
218 6b shows a 10-member combination consistent with our 18-member mean response ( $\Delta T = 0.03$  °C). 6c and 6d  
219 show 10-member combinations with  $\Delta T$  at the edges of, but still within, the 9-95% confidence interval ( $\Delta T = \pm 0.05$   
220 °C).

221

222 While panels b-d of Figure 6 all represent deliberate picking of ensemble members, the analysis illustrates how,  
223 even with a decently sized ensemble of 10 members, one could conclude that the IMO shipping regulations may  
224 lead to substantial global mean warming or global mean cooling. This illustrates the importance of internal climate  
225 variability in detecting a global mean temperature response associated with the IMO shipping regulations, and the  
226 importance of a sufficiently large ensemble size to reduce the risk of spurious conclusions. We note that our choice

Deleted: .

228 of 18 ensemble members, as with most experimental designs, also represents a trade-off between additional  
229 information gained versus increased computational expense. Clearly, however, a moderately large ensemble size  
230 of 10—which has been shown to be sufficient in some contexts (e.g. Monerie et al., 2022)—is not sufficient to  
231 make robust claims regarding the impact of shipping SO<sub>2</sub> reductions on global mean temperature, in particular  
232 during its early transient evolution.

233

#### 234 **Discussion and conclusions**

235 The strict new fuel regulations introduced by the IMO provided a valuable experiment to better understand the  
236 role of changing anthropogenic aerosol in the climate system, particularly as an analogue to other, current and  
237 future, efforts to improve air quality globally. Using an 18-member ensemble of simulations from CESM2, we  
238 find that the global temperature response to the IMO regulations that came into force in 2020 is +0.03 °C, with a  
239 5-95% confidence range of [-0.09, 0.19], for the period 2020-2040. This result, which is consistent with a null  
240 hypothesis of no discernible global mean temperature response, is at the low end of other estimates of this warming  
241 effect, from simple energy balance models (Gettelman et al., 2024; Yuan et al., 2024) and global climate models  
242 (Quaglia & Visioni, 2024; Yoshioka et al., 2024), which suggested global warming between 0.04 °C (Yoshioka et  
243 al., 2024) and 0.2 °C (Quaglia & Visioni, 2024) associated with the shipping regulations over decadal timescales.  
244 To understand the differences between these conclusions and to explain why our analysis provides an important  
245 bound on the role of shipping emissions changes in recently observed temperature extremes, it is necessary to  
246 discuss in some detail the methodologies and framings behind the other results.

247

Deleted: )

249 Some recent studies of the climate impact of the IMO regulations used EBMs to calculate the global temperature  
250 response from the effective radiative forcing (Gettelman et al., 2024; Yuan et al., 2024). These simple models are  
251 useful in many situations, notably for comparing the climate implications of known emissions from industrial  
252 sectors, regions or scenarios. However for absolute climate impacts they require substantial assumptions to be  
253 made about the sensitivity and timescale of the responses, and – critically - do not account for regional  
254 heterogeneity of responses or climate feedbacks such as influences on ocean circulation or sea ice, or internal  
255 variability. Ocean feedbacks may be particularly important in the case of shipping emission changes which are  
256 focussed over the Northern Hemisphere oceans, where it is conceivable that the ocean mixed layers may warm  
257 more efficiently than e.g. the Southern Ocean (e.g. Ma et al., 2020). Region-specific cloud responses and  
258 teleconnections to aerosol changes over Northern Hemisphere oceans may also differ from those to e.g. sulphur  
259 emission changes in Asia (Burney et al., 2022; Persad & Caldeira, 2018), which tend to dominate the total global  
260 response to recent sulphur emission changes used to calibrate simple EBMs. Coupled climate models provide  
261 estimates of the temperature response to the IMO regulations that take such feedbacks and pattern dependencies  
262 into account.

263

264 Despite the differences in the approach, our estimate of the global warming due to the IMO regulations is similar  
265 to Gettelman et al. (2024)'s estimate of 0.07 °C by 2030, which is based on the FaIR EBM. The EBM approach  
266 taken by Yuan et al. (2024), however, which diagnoses a global temperature anomaly of 0.17 °C at equilibrium  
267 overstates the response to their forcing by a factor of 1.4. This is because Yuan et al. (2024) calculate a global  
268 temperature response using a global climate feedback parameter, but using an ocean-area mean ERF. A global  
269 feedback parameter should be used with a global forcing in this context, which would reduce their forcing and  
270 temperature estimates by a factor of 0.7, the fraction of global area that is ocean, from 0.2 W m<sup>-2</sup> to 0.14 W m<sup>-2</sup>

Deleted:

272 and 0.17 °C to 0.12 °C in equilibrium, respectively. Uncertainty in the climate feedback parameter should also be  
273 considered in this estimate. Using a feedback parameter equivalent to that of CO<sub>2</sub>, the AR6 likely range for ECS  
274 of 2.5-4.0 °C (which may both be oversimplistic assumptions), and 2xCO<sub>2</sub> forcing of 3.9±0.5 W m<sup>-2</sup> (90% range)  
275 would produce an equilibrium warming due to a forcing of 0.14 W m<sup>-2</sup> of 0.09-0.14 °C (90% range). Seven years,  
276 the timescale used by Yuan et al. (2024) in their calculation, is approximately the time taken for the upper-ocean  
277 to reach equilibrium, so, based on Gregory et al. (2024), one would expect to see around two thirds of the  
278 equilibrium response (i.e. 0.06-0.10 °C) in that time. With these factors taken into account, the estimate presented  
279 by Yuan et al. (2024) would have been consistent with those of Gettelman et al. (2024), and those presented in this  
280 work.

281

282 ESM estimates of the temperature response to the IMO regulations initially appear to show similar diversity to  
283 those based on EBMs. However, this can be seen to largely be due to a difference in the framing of the experiments  
284 and reporting of the results, rather than a substantive difference in the main conclusions. Using HadGEM3-GC3.1-  
285 LL, Yoshioka et al. (2024) estimated a global mean warming of 0.04 °C (averaged over 2020-2049), which is in  
286 agreement with our estimate of 0.03 [-0.09,0.19] °C (averaged over 2020-2040). Their model has a similar ERF  
287 of 0.13 Wm<sup>-2</sup>, and they use coupled transient simulations with 12 ensemble members per experiment. Their global  
288 mean warming estimate is similar to that presented in this study, but the pattern of warming is markedly different,  
289 with most of the significant warming over SE Asia and the East Pacific. Conversely, Quaglia & Vioni (2024)  
290 estimate a temperature increase of 0.2 °C by 2030 due to the introduction of the IMO regulations. They use the  
291 same model that we have used in this study, and a similar experiment design, with transient simulations initialised  
292 from the CESM2 Large Ensemble. Although their temperature response is an order of magnitude larger than our  
293 stated response, it is not inconsistent with our results. We show in Figure 3a that the global temperature response

Deleted: .

295 to the reduction of shipping emissions peaks in 2029 at 0.16 [-0.17, 0.52] °C. Our best estimate of the warming by  
296 2030 is 0.07 [-0.14, 0.28] °C, where the range is  $\pm 1$  standard deviation and encompasses a warming of 0.2 °C.  
297 However, our 18-member ensemble shows that the global ensemble mean warming over 2020-2040 is not  
298 statistically significantly different from zero ( $p=0.18$ ), even in 2030 ( $p=0.054$ ).  
299  
300 The apparently large discrepancy between our CESM2 numbers and those from Quaglia & Vioni (2024) also  
301 demonstrates the importance of framing. We report a 2020-2040 mean value, and they report the value for 2030.  
302 Both our Figure 3a and Yoshioka et al. (2024)'s Figure 6 show that the maximum global temperature response to  
303 the 2020 emissions change occurs around 2030, and the estimate of the temperature response by 2030 is consistent  
304 across all three studies. Yoshioka et al. (2024) also find a long-term mean response of 0.04 °C, averaged over  
305 2020-2049, which is more consistent with our estimate of 0.03 °C. However, while we show in Figure 3a that the  
306 global warming in response to the IMO regulations is not significant, Yoshioka et al. (2024) present significant  
307 decadal mean warming in their Figure 6. However, this is based on  $\pm 1$  standard error (SE), while we show  $\pm 1$   
308 standard deviation. Yoshioka et al. (2024) use 12 members, so their standard deviation of  $\sqrt{12} * SE$  would also  
309 indicate that these decadal mean values were always within one standard deviation of 0, consistent with our results.  
310  
311 Using large ensembles of simulations differing only by the initial conditions is an important technique for  
312 distinguishing forced responses from internal variability, particularly when looking for regional responses, or  
313 considering small forcings. Here, our large ensemble confirms that the global response to IMO regulations in  
314 CESM2 cannot be distinguished from internal variability, at least in terms of global mean surface temperature.  
315 Our best estimate is not significantly different from zero, and subsampling our 18-member ensemble to produce  
316 estimates of the global temperature response based on different ensemble sizes always returns a mean estimate

317 that is not significantly different from 0 at the 5% level. In fact, given the ensemble variance and the number of  
318 simulations available, the minimum detectable effect size over the full 20 years at a significance level of 0.05 is  
319 approximately 0.048 °C. The warming due to the ship emissions changes in CESM2 is therefore very likely less  
320 than 0.05 °C. A 10-member ensemble, as used by Quaglia & Visionsi (2024), can only significantly detect an effect  
321 larger than 0.07 °C. To demonstrate this, 10 members sub-sampled from within our 18-member ensemble, can  
322 give a global warming estimate of 0.05 °C or a global cooling of 0.05 °C, averaged over 2020-2040.

323

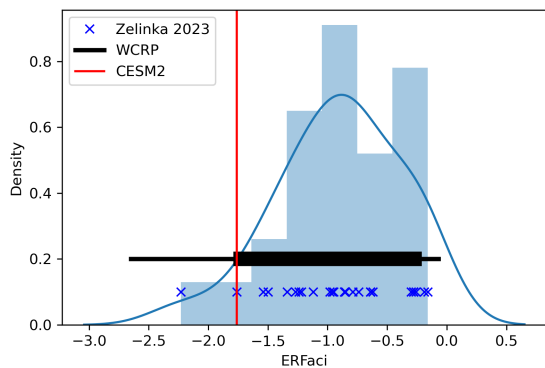
324 Large ensembles also make it possible to characterise the spatial pattern of the response, and identify physically  
325 robust responses that are consistent across ensemble members. North Atlantic, Greenland Iceland and Norwegian  
326 (GIN) seas, South Atlantic, and East Pacific warming are common features of all our subsampled ensembles.  
327 However, only the North Atlantic and GIN sea warming are physically robust in addition to being significant at  
328 the 5% level. The difference between the pattern of warming shown in this work and by Yoshioka et al. (2024)  
329 likely has a large component of internal variability, in addition to the effects of structural differences between the  
330 models used.

331

332 Our results highlight the challenge in rapidly attributing observed extreme events to evolving or temporary  
333 anthropogenic changes, particularly given the large internal climate variability on annual-to-decadal timescales.  
334 By crowd-sourcing computing resources we were able to rapidly generate an ensemble of fully coupled Earth  
335 System Model simulations of sufficient size to quantify the forced response and its confidence interval. However,  
336 this highlights a deficiency in current medium term climate attribution tasks. As climate change is broadly  
337 acknowledged to be increasingly contributing to the extreme events experienced by millions of people around the  
338 world, climate scientists are increasingly tasked with understanding and accurately attributing them - but the

339 resources to conduct this at scale are limited and ad-hoc. An operational climate body that was specifically tasked  
340 with running decadal-scale attribution studies (Stevens 2024), or the development of trusted methods for separating  
341 forced signals from variability (Samset et al. 2022), would provide a valuable resource as the demand for such  
342 information accelerates. The IMO shipping regulations do lead to a relatively small forced global mean surface  
343 warming in on our results, consistent with its moderate aerosol ERF, and also with a zero response when internal  
344 variability is taken into account. However, we note that other, future and ongoing, broader aerosol emission  
345 reductions — although uncertain (Persad et al., 2023) — are expected to lead to a much larger aerosol ERF (e.g.,  
346 Wilcox et al., 2023) and may thus still drive significant global warming and regional climate change impacts (e.g.,  
347 Allen et al., 2020; Allen et al., 2021).

348 **Figures**

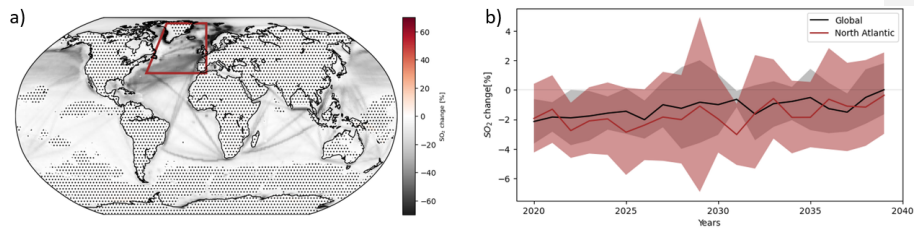


349



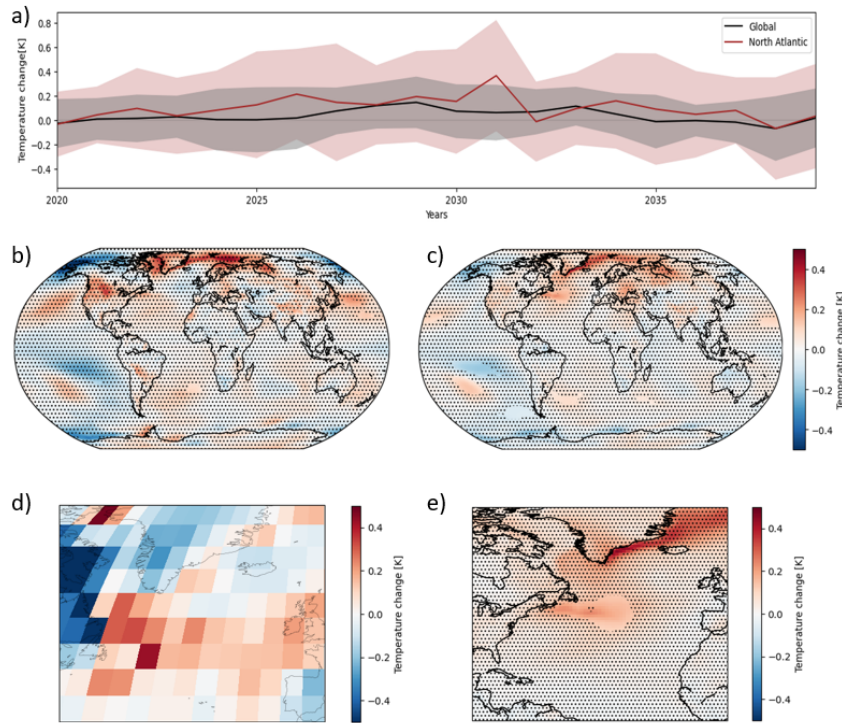
350 **Figure 1: Distribution of the effective radiative forcing due to aerosol cloud interactions (ERFaci) in CMIP6 models as**  
351 **assessed by Zelinka et al. (2023) in blue, and Bellouin et al. 2020 in black, with CESM2 highlighted in red.**

352



353

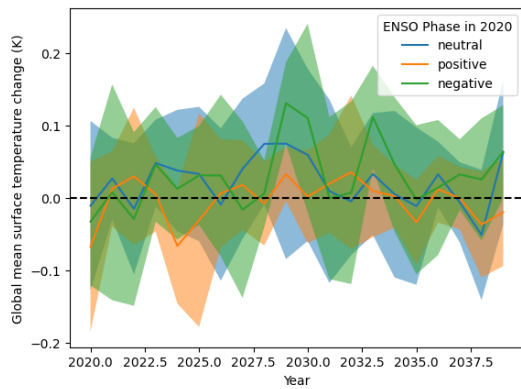
354 **Figure 2: a) Relative change in SO<sub>2</sub> near the surface due to the shipping emissions perturbation, averaged over the**  
355 **whole 2020-2040 period, where stippling represents locations where the null hypothesis of 'no change' cannot be**  
356 **rejected at P < 0.05. b) Annual mean evolution of SO<sub>2</sub>, averaged over the entire globe (black line; shading shows +/- one**  
357 **standard deviation in ensemble member spread) and over the North Atlantic region (red line) as indicated on the map.**  
358 **All changes are relative to the baseline Shared Socioeconomic Pathway 3-7.0 (SSP370).**



359

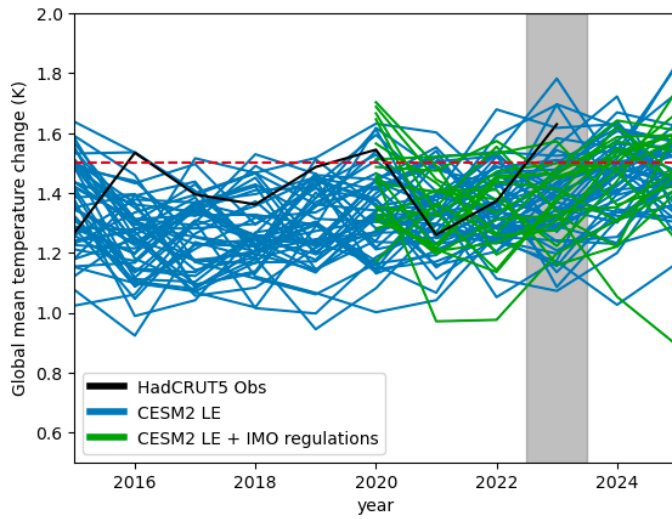
360 **Figure 3: a) Global and North Atlantic annual mean evolution in temperature change (shading shows +/- one standard**  
 361 **deviation in ensemble member spread); b) Annual mean temperature change for 2020-2025; c) Annual mean**  
 362 **temperature change for 2020-2040; d) Observed anomalous warming in North Atlantic sea-surface temperature in**  
 363 **2023; e) A close-up of (c) showing the corresponding region of the North Atlantic. Stippling in b,c,e represents locations**  
 364 **where the null hypothesis of 'no change' cannot be rejected at  $P < 0.05$ . All changes are relative to the corresponding**  
 365 **baseline CESM2 LENS simulations of SSP370.**

366



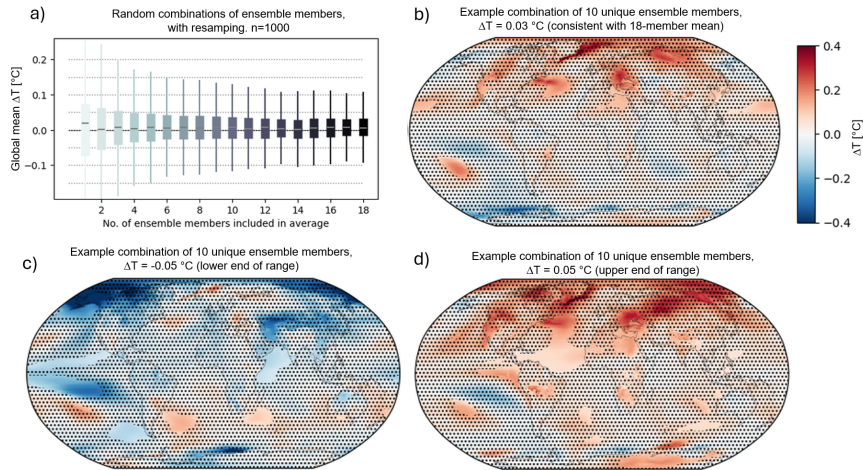
367

368 **Figure 4: Global mean change in surface temperature due to shipping emissions changes with respect to the baseline**  
369 **SSP370 simulations, subdivided into three ENSO phases in 2020: neutral (blue; 8 members); positive (orange; 5**  
370 **members); negative (green; 5 members). Shading shows the inter-member spread, represented by +/- one standard**  
371 **deviation.**



372

373 **Figure 5: Global mean surface temperature change with respect to piControl for the baseline historical + SSP370**  
 374 **CESM2 LENS ensemble (blue) and the perturbed shipping emissions ensemble performed in this study (green), overlaid**  
 375 **on the HadCRUT SST observational estimate (with respect to the 1850-1900 average; black). The year 2023 is**  
 376 **highlighted. The red dashed line represents the 1.5°C Paris agreement warming threshold.**



377  
 378 **Figure 6: Ensemble size is crucial for quantifying a forced signal for weak perturbations. (a) Spread in 2020-2040 global,**  
 379 **annual mean surface temperature change ( $\Delta T$ ) when randomly sampling and averaging  $N$  (given on the x-axis) ensemble**  
 380 **members out of the total of 18 available members 1000 times, with resampling. Each spread includes 1000 combinations,**  
 381 **illustrating an increasing robustness of  $\Delta T$  as number of ensemble members. Boxes show the median and 5-95% range,**  
 382 **whiskers show the maximum and minimum values. (b) Example combination of 10 ensemble members, where the**  
 383 **global, annual mean  $\Delta T$  is consistent with the 18-member mean ( $\Delta T = 0.03$  °C). Hatching shows grid points not**  
 384 **significant at the 95% confidence level, as for Figure 2. (c) As panel (c), but for an example combination consistent with**  
 385  **$\Delta T$  at the lower end of the 10-member mean range. ( $\Delta T = -0.05$  °C). (d) As panel (c), but for an example combination**  
 386 **consistent with  $\Delta T$  at the upper end of the 10-member mean range. ( $\Delta T = 0.05$  °C).**

387

388 **Competing Interests**

389 At least one of the (co-)authors is a member of the editorial board of Atmospheric Chemistry and Physics.  
390

391 **Acknowledgements**

392 Part of the simulations were enabled by resources provided by the National Academic Infrastructure for  
393 Supercomputing in Sweden (NAISS), partially funded by the Swedish Research Council through grant agreement  
394 no. 2022-06725. B.H.S, C.W.S, L.J.W. and M.T.L. acknowledge funding by the Research Council of Norway  
395 through projects CATHY (324182), and support by the Center for Advanced Study in Oslo, Norway that funded  
396 and hosted the HETCLIF centre during the academic year of 2023/24. C.W.S. is also supported by the Research  
397 Council of Norway through the ACCEPT project (315195). G.P acknowledges support from the U.S. National  
398 Science Foundation under AGS-CLD Award #2235177. A.M.L.E acknowledges support from the European  
399 Union's Horizon 2020 research and innovation programme (FORCeS, grant no. 821205). R.J.A. is supported by  
400 NSF grant AGS-2153486. We would like to acknowledge high-performance computing support from Cheyenne  
401 (doi:10.5065/D6RX99HX) provided by the NCAR-Wyoming Supercomputing Center, sponsored by the National  
402 Science Foundation and the State of Wyoming and supported by NCAR's Computational and Information Systems  
403 Laboratory using allocation WYOM0182. The authors are grateful to Jonathan Gregory for discussions that  
404 strengthened this manuscript.

405

406

407

408

409

410

411

412

413

414 **References**

415

416 Albrecht, B. A. (1989). Aerosols, Cloud Microphysics, and Fractional Cloudiness. *Science*, *245*(4923), 1227–

417 1230. <https://doi.org/10.1126/science.245.4923.1227>

418 Bellouin, N., Quaas, J., Gryspeerdt, E., Kinne, S., Stier, P., Watson-Parris, D., Boucher, O., Carslaw, K. S.,

419 Christensen, M., Daniau, A.-L., Dufresne, J.-L., Feingold, G., Fiedler, S., Forster, P., Gettelman, A.,

420 Haywood, J. M., Lohmann, U., Malavelle, F., Mauritsen, T., ... Stevens, B. (2020). Bounding Global

421 Aerosol Radiative Forcing of Climate Change. *Reviews of Geophysics*, *58*(1), e2019RG000660.

422 <https://doi.org/10.1029/2019RG000660>

423 Bogenschutz, P. A., Gettelman, A., Hannay, C., Larson, V. E., Neale, R. B., Craig, C., & Chen, C.-C. (2018). The

424 path to CAM6: coupled simulations with CAM5.4 and CAM5.5. *Geoscientific Model Development*, *11*(1),

425 235–255. <https://doi.org/10.5194/gmd-11-235-2018>

426 Burney, J., Persad, G., Proctor, J., Bendavid, E., Burke, M., & Heft-Neal, S. (2022). Geographically resolved social

427 cost of anthropogenic emissions accounting for both direct and climate-mediated effects. *Science Advances*,

428 *8*(38), eabn7307. <https://doi.org/10.1126/sciadv.abn7307>

429 Christensen, M. W., Gettelman, A., Cermak, J., Dagan, G., Diamond, M., Douglas, A., Feingold, G., Glassmeier,

430 F., Goren, T., Grosvenor, D. P., Gryspeerdt, E., Kahn, R., Li, Z., Ma, P. L., Malavelle, F., McCoy, I. L.,

431 McCoy, D. T., McFarquhar, G., Mülmenstädt, J., ... Yuan, T. (2022). Opportunistic experiments to constrain  
432 aerosol effective radiative forcing. *Atmospheric Chemistry and Physics*, 22(1), 641–674.  
433 <https://doi.org/10.5194/acp-22-641-2022>

434 Danabasoglu, G., Bates, S. C., Briegleb, B. P., Jayne, S. R., Jochum, M., Large, W. G., Peacock, S., & Yeager, S.  
435 G. (2012). The CCSM4 Ocean Component. *Journal of Climate*, 25(5), 1361–1389.  
436 <https://doi.org/10.1175/JCLI-D-11-00091.1>

437 Danabasoglu, G., Lamarque, J.-F., Bacmeister, J., Bailey, D. A., DuVivier, A. K., Edwards, J., Emmons, L. K.,  
438 Fasullo, J., Garcia, R., Gettelman, A., Hannay, C., Holland, M. M., Large, W. G., Lauritzen, P. H., Lawrence,  
439 D. M., Lenaerts, J. T. M., Lindsay, K., Lipscomb, W. H., Mills, M. J., ... Strand, W. G. (2020). The  
440 Community Earth System Model Version 2 (CESM2). *Journal of Advances in Modeling Earth Systems*,  
441 12(2), e2019MS001916. <https://doi.org/https://doi.org/10.1029/2019MS001916>

442 Deser, C., Knutti, R., Solomon, S., & Phillips, A. S. (2012). Communication of the role of natural variability in  
443 future North American climate. *Nature Climate Change*, 2(11), 775–779.  
444 <https://doi.org/10.1038/nclimate1562>

445 Deser, C., Lehner, F., Rodgers, K. B., Ault, T., Delworth, T. L., DiNezio, P. N., Fiore, A., Frankignoul, C., Fyfe,  
446 J. C., Horton, D. E., Kay, J. E., Knutti, R., Lovenduski, N. S., Marotzke, J., McKinnon, K. A., Minobe, S.,  
447 Randerson, J., Screen, J. A., Simpson, I. R., & Ting, M. (2020). Insights from Earth system model initial-  
448 condition large ensembles and future prospects. *Nature Climate Change*, 10(4), 277–286.  
449 <https://doi.org/10.1038/s41558-020-0731-2>

450 Diamond, M. S. (2023). Detection of large-scale cloud microphysical changes within a major shipping corridor  
451 after implementation of the International Maritime Organization 2020 fuel sulfur regulations. *Atmospheric*  
452 *Chemistry and Physics*, 23(14), 8259–8269. <https://doi.org/10.5194/acp-23-8259-2023>



453 Emmons, L. K., Schwantes, R. H., Orlando, J. J., Tyndall, G., Kinnison, D., Lamarque, J.-F., Marsh, D., Mills, M.  
454 J., Tilmes, S., Bardeen, C., Buchholz, R. R., Conley, A., Gettelman, A., Garcia, R., Simpson, I., Blake, D.  
455 R., Meinardi, S., & Pétron, G. (2020). The Chemistry Mechanism in the Community Earth System Model  
456 Version 2 (CESM2). *Journal of Advances in Modeling Earth Systems*, 12(4), e2019MS001882.  
457 <https://doi.org/10.1029/2019MS001882>

458 Fasullo, J. T., Lamarque, J.-F., Hannay, C., Rosenbloom, N., Tilmes, S., DeRepentigny, P., Jahn, A., & Deser, C.  
459 (2022). Spurious Late Historical-Era Warming in CESM2 Driven by Prescribed Biomass Burning  
460 Emissions. *Geophysical Research Letters*, 49(2), e2021GL097420. <https://doi.org/10.1029/2021GL097420>

461 Fasullo, J. T., Rosenbloom, N., & Buchholz, R. (2023). A multiyear tropical Pacific cooling response to recent  
462 Australian wildfires in CESM2. *Science Advances*, 9(19), eadg1213. <https://doi.org/10.1126/sciadv.adg1213>

463 Forster, P., Storelvmo, T., Armour, K., Collins, W., Dufresne, J.-L., Frame, D., Lunt, D., Mauritsen, T., Palmer,  
464 M., & Watanabe, M. (2021). The Earth's energy budget, climate feedbacks, and climate sensitivity. *Climate  
465 Change 2021: The Physical Science Basis. Contribution of Working Group I to the Sixth Assessment Report  
466 of the Intergovernmental Panel on Climate Change*, 923–1054. <https://doi.org/10.1017/9781009157896.009>

467 Gettelman, A., & Morrison, H. (2015). Advanced Two-Moment Bulk Microphysics for Global Models. Part I:  
468 Off-Line Tests and Comparison with Other Schemes. *Journal of Climate*, 28(3), 1268–1287.  
469 <https://doi.org/10.1175/JCLI-D-14-00102.1>

470 Gettelman, A., Christensen, M. W., Diamond, M. S., Gryspeerdt, E., Manshausen, P., Stier, P., Watson-Parris,  
471 D., Yang, M., Yoshioka, M., Yuan, T.: Has Reducing Ship Emissions Brought Forward Global Warming?  
472 *Geophysical Review Letters* (under review)

473 Glassmeier, F., Hoffmann, F., Johnson, J. S., Yamaguchi, T., Carslaw, K. S., & Feingold, G. (2021). Aerosol-  
474 cloud-climate cooling overestimated by ship-track data. *Science*, 371(6528), 485–489.  
475 <https://doi.org/doi:10.1126/science.abd3980>

476 Hassan, T., Allen, R. J., Liu, W., & Randles, C. A. (2021). Anthropogenic aerosol forcing of the Atlantic  
477 meridional overturning circulation and the associated mechanisms in CMIP6 models. *Atmospheric*  
478 *Chemistry and Physics*, 21(8), 5821–5846. <https://doi.org/10.5194/acp-21-5821-2021>

479 Hunke, E. C., Lipscomb, W. H., Turner, A. K., Jeffery, N., & Elliott, S. (2015). CICE: the Los Alamos Sea Ice  
480 Model Documentation and Software User’s Manual Version 5. *Los Alamos National Laboratory Technical*  
481 *Report, LA-CC-06-012*.

482 IMO: IMO 2020: Consistent Implementation of MARPOL Annex VI. International Maritime Organization, 2019

483 Kay, J. E., Deser, C., Phillips, A., Mai, A., Hannay, C., Strand, G., Arblaster, J. M., Bates, S. C., Danabasoglu, G.,  
484 Edwards, J., Holland, M., Kushner, P., Lamarque, J.-F., Lawrence, D., Lindsay, K., Middleton, A., Munoz,  
485 E., Neale, R., Oleson, K., ... Vertenstein, M. (2015). The Community Earth System Model (CESM) Large  
486 Ensemble Project: A Community Resource for Studying Climate Change in the Presence of Internal Climate  
487 Variability. *Bulletin of the American Meteorological Society*, 96(8), 1333–1349.  
488 <https://doi.org/10.1175/BAMS-D-13-00255.1>

489 Kirchmeier-Young, M. C., Zwiers, F. W., & Gillett, N. P. (2017). Attribution of Extreme Events in Arctic Sea Ice  
490 Extent. *Journal of Climate*, 30(2), 553–571. <https://doi.org/10.1175/JCLI-D-16-0412.1>

491 Lawrence, D. M., Fisher, R. A., Koven, C. D., Oleson, K. W., Swenson, S. C., Bonan, G., Collier, N., Ghimire,  
492 B., van Kampenhou, L., Kennedy, D., Kluzek, E., Lawrence, P. J., Li, F., Li, H., Lombardozzi, D., Riley,  
493 W. J., Sacks, W. J., Shi, M., Vertenstein, M., ... Zeng, X. (2019). The Community Land Model Version 5:

494 Description of New Features, Benchmarking, and Impact of Forcing Uncertainty. *Journal of Advances in*  
495 *Modeling Earth Systems*, 11(12), 4245–4287. <https://doi.org/10.1029/2018MS001583>

496 Li, C., McLinden, C., Fioletov, V., Krotkov, N., Carn, S., Joiner, J., Streets, D., He, H., Ren, X., Li, Z., &  
497 Dickerson, R. R. (2017). India Is Overtaking China as the World’s Largest Emitter of Anthropogenic Sulfur  
498 Dioxide. *Scientific Reports*, 7(1), 14304. <https://doi.org/10.1038/s41598-017-14639-8>

499 Liu, X., Ma, P. L., Wang, H., Tilmes, S., Singh, B., Easter, R. C., Ghan, S. J., & Rasch, P. J. (2016). Description  
500 and evaluation of a new four-mode version of the Modal Aerosol Module (MAM4) within version 5.3 of the  
501 Community Atmosphere Model. *Geoscientific Model Development*, 9(2), 505–522.  
502 <https://doi.org/10.5194/gmd-9-505-2016>

503 Ma, X., Liu, W., Allen, R. J., Huang, G., & Li, X. (2020). Dependence of regional ocean heat uptake on  
504 anthropogenic warming scenarios. *Science Advances*, 6(45). <https://doi.org/10.1126/sciadv.abc0303>

505 Maher, N., Milinski, S., Suarez-Gutierrez, L., Botzet, M., Dobrynin, M., Kornblueh, L., Kröger, J., Takano, Y.,  
506 Ghosh, R., Hedemann, C., Li, C., Li, H., Manzini, E., Notz, D., Putrasahan, D., Boysen, L., Claussen, M.,  
507 Ilyina, T., Olonscheck, D., ... Marotzke, J. (2019). The Max Planck Institute Grand Ensemble: Enabling the  
508 Exploration of Climate System Variability. *Journal of Advances in Modeling Earth Systems*, 11(7), 2050–  
509 2069. <https://doi.org/10.1029/2019MS001639>

510 Monerie, P.-A., Wilcox, L. J., & Turner, A. G. (2022). Effects of Anthropogenic Aerosol and Greenhouse Gas  
511 Emissions on Northern Hemisphere Monsoon Precipitation: Mechanisms and Uncertainty. *Journal of*  
512 *Climate*, 35(8), 2305–2326. <https://doi.org/10.1175/JCLI-D-21-0412.1>

513 Morice, C. P., Kennedy, J. J., Rayner, N. A., Winn, J. P., Hogan, E., Killick, R. E., Dunn, R. J. H., Osborn, T. J.,  
514 Jones, P. D., & Simpson, I. R. (2021). An Updated Assessment of Near-Surface Temperature Change From

515 1850: The HadCRUT5 Data Set. *Journal of Geophysical Research: Atmospheres*, 126(3).  
516 <https://doi.org/10.1029/2019JD032361>

517 O'Neill, B. C., Tebaldi, C., Vuuren, D. P. van, Eyring, V., Friedlingstein, P., Hurtt, G., Knutti, R., Kriegler, E.,  
518 Lamarque, J.-F., Lowe, J., Meehl, G. A., Moss, R., Riahi, K., & Sanderson, B. M. (2016). The Scenario  
519 Model Intercomparison Project (ScenarioMIP) for CMIP6. *Geoscientific Model Development*, 9(9), 3461–  
520 3482. <https://doi.org/https://doi.org/10.5194/gmd-9-3461-2016>

521 Persad, G. G., & Caldeira, K. (2018). Divergent global-scale temperature effects from identical aerosols emitted  
522 in different regions. *Nat Commun*, 9(1), 3289. <https://doi.org/10.1038/s41467-018-05838-6>

523 Quaglia, I., & Visioni, D. (2024). Modeling 2020 regulatory changes in international shipping emissions helps  
524 explain 2023 anomalous warming. *EGUsphere*, 1–19. <https://doi.org/10.5194/egusphere-2024-1417>

525 Rodgers, K. B., Lee, S.-S., Rosenbloom, N., Timmermann, A., Danabasoglu, G., Deser, C., Edwards, J., Kim, J.-  
526 E., Simpson, I. R., Stein, K., Stuecker, M. F., Yamaguchi, R., Bódai, T., Chung, E.-S., Huang, L., Kim, W.  
527 M., Lamarque, J.-F., Lombardozzi, D. L., Wieder, W. R., & Yeager, S. G. (2021). Ubiquity of human-  
528 induced changes in climate variability. *Earth System Dynamics*, 12(4), 1393–1411.  
529 <https://doi.org/10.5194/esd-12-1393-2021>

530 Samset, B. H., Lund, M. T., Bollasina, M., Myhre, G., & Wilcox, L. (2019). Emerging Asian aerosol patterns.  
531 *Nature Geoscience*, 12(8), 582–584. <https://doi.org/10.1038/s41561-019-0424-5>

532 Schlund, M., Lauer, A., Gentine, P., Sherwood, S. C., & Eyring, V. (2020). Emergent constraints on equilibrium  
533 climate sensitivity in CMIP5: do they hold for CMIP6? *Earth System Dynamics*, 11(4), 1233–1258.  
534 <https://doi.org/10.5194/esd-11-1233-2020>

535 Schmidt, G. (2024). Climate models can't explain 2023's huge heat anomaly — we could be in uncharted territory.  
536 *Nature*, 627(8004), 467. <https://doi.org/10.1038/d41586-024-00816-z>

537 Shindell, D., & Faluvegi, G. (2009). Climate response to regional radiative forcing during the twentieth century.  
538 *Nature Geoscience*, 2(4), 294–300. <https://doi.org/10.1038/ngeo473>

539 Simpson, I. R., Rosenbloom, N., Danabasoglu, G., Deser, C., Yeager, S. G., McCluskey, C. S., Yamaguchi, R.,  
540 Lamarque, J.-F., Tilmes, S., Mills, M. J., & Rodgers, K. B. (2023). The CESM2 Single-Forcing Large  
541 Ensemble and Comparison to CESM1: Implications for Experimental Design. *Journal of Climate*, 36(17),  
542 5687–5711. <https://doi.org/10.1175/JCLI-D-22-0666.1>

543 Skeie, R. B., Byrom, R., Hodnebrog, Ø., Jouan, C., & Myhre, G. (2024). Multi-model effective radiative forcing  
544 of the 2020 sulphur cap for shipping. *EGUsphere*, 1–14. <https://doi.org/10.5194/egusphere-2024-1394>

545 Stevens, B., & Feingold, G. (2009). Untangling aerosol effects on clouds and precipitation in a buffered system.  
546 *Nature*, 461(7264), 607–613. <https://doi.org/10.1038/nature08281>

547 Twomey, S. (1974). Pollution and the planetary albedo. *Atmospheric Environment (1967)*, 8(12), 1251–1256.  
548 <http://www.sciencedirect.com/science/article/pii/0004698174900043>

549 van der A, R. J., Mijling, B., Ding, J., Koukouli, M. E., Liu, F., Li, Q., Mao, H., & Theys, N. (2017). Cleaning up  
550 the air: effectiveness of air quality policy for SO<sub>2</sub> and NO<sub>x</sub> emissions in China. *Atmospheric Chemistry and*  
551 *Physics*, 17(3), 1775–1789. <https://doi.org/10.5194/acp-17-1775-2017>

552 Wall, C. J., Norris, J. R., Possner, A., McCoy, D. T., McCoy, I. L., & Lutsko, N. J. (2022). Assessing effective  
553 radiative forcing from aerosol–cloud interactions over the global ocean. *Proceedings of the National*  
554 *Academy of Sciences*, 119(46), e2210481119. <https://doi.org/10.1073/pnas.2210481119>

555 Wang, G., Cai, W., Santoso, A., Wu, L., Fyfe, J. C., Yeh, S.-W., Ng, B., Yang, K., & McPhaden, M. J. (2022).  
556 Future Southern Ocean warming linked to projected ENSO variability. *Nature Climate Change*, 12(7), 649–  
557 654. <https://doi.org/10.1038/s41558-022-01398-2>

558 Watson-Parris, D., Christensen, M. W., Laursen, A., Clewley, D., Gryspeerdt, E., & Stier, P. (2022). Shipping  
559 regulations lead to large reduction in cloud perturbations. *Proceedings of the National Academy of Sciences*,  
560 *119*(41), e2206885119. <https://doi.org/10.1073/pnas.2206885119>

561 Watson-Parris, D., & Smith, C. J. (2022). Large uncertainty in future warming due to aerosol forcing. *Nature*  
562 *Climate Change*, *12*(12), 1111–1113. <https://doi.org/10.1038/s41558-022-01516-0>

563 Westervelt, D. M., Mascioli, N. R., Fiore, A. M., Conley, A. J., Lamarque, J.-F., Shindell, D. T., Faluvegi, G.,  
564 Previdi, M., Correa, G., & Horowitz, L. W. (2020). Local and remote mean and extreme temperature  
565 response to regional aerosol emissions reductions. *Atmospheric Chemistry and Physics*, *20*(5), 3009–3027.  
566 <https://doi.org/https://doi.org/10.5194/acp-20-3009-2020>

567 Yoshioka, M., Grosvenor, D. P., Booth, B. B. B., Morice, C. P., & Carslaw, K. S. (2024). Warming effects of  
568 reduced sulfur emissions from shipping. *EGUsphere*, 1–19. <https://doi.org/10.5194/egusphere-2024-1428>

569 Yuan, T., Song, H., Oreopoulos, L., Wood, R., Bian, H., Breen, K., Chin, M., Yu, H., Barahona, D., Meyer, K., &  
570 Platnick, S. (2024). Abrupt reduction in shipping emission as an inadvertent geoengineering termination  
571 shock produces substantial radiative warming. *Communications Earth & Environment*, *5*(1), 1–8.  
572 <https://doi.org/10.1038/s43247-024-01442-3>

573 Zelinka, M. D., Smith, C. J., Qin, Y., & Taylor, K. E. (2023). Comparison of methods to estimate aerosol effective  
574 radiative forcings in climate models. *Atmospheric Chemistry and Physics*, *23*(15), 8879–8898.  
575 <https://doi.org/10.5194/acp-23-8879-2023>

576  
577  
578